Polyacrylamide brushes with varied morphologies as a tool for control of the intermolecular interactions within EPDM/MVQ blends

Monika Galeziewska[1], Magdalena Lipinska[1], Miroslav Mrlik[2], Marketa Ilcikova[1,3*], Veronika Gajdosova[4], Miroslav Slouf[4], Eva Achbergerová[5], Lenka Musilová[6], Jaroslav Mosnacek[3,7], Joanna Pietrasik[1*]

[1] Lodz University of Technology, Department of Chemistry, Institute of Polymer and Dye Technology, Stefanowskiego 12/16, 90 924 Lodz, Poland

[2] Tomas Bata University in Zlin, University Institute, Centre of Polymer Systems, Trida T. Bati 5678, Zlin 76001, Czech Republic

[3] Polymer Institute, Slovak Academy of Sciences, Dubravska cesta 9, 845 41 Bratislava, Slovakia

[4] Institute of Macromolecular Chemistry, Czech Academy of Sciences, Heyrovskeho namesti 2, 162 06 Praha 6, Czech Republic

[5] CEBIA-Tech, Faculty of Applied Informatics, Tomas Bata University in Zlín, Nad Stráněmi 4511, 760 05 Zlín, Czech Republic

[6] Department of Physics and Materials Engineering, Faculty of Technology, Tomas Bata University in Zlin, Vavrečkova 5569, 760 01 Zlín, Czech Republic

[7] Centre for Advanced Materials Application, Slovak Academy of Sciences, Dubravska cesta 9, 845 11 Bratislava, Slovakia

monika.galeziewska@dokt.p.lodz.pl, magdalena.lipinska@p.lodz.pl, mrlik@utb.cz, marketa.ilcikova@savba.sk, gajdosova@imc.cas.cz, slouf@imc.cas.cz, jaroslav.mosnacek@savba.sk, joanna.pietrasik@p.lodz.pl, achbergerova@utb.cz, musilova@utb.cz

Corresponding authors: joanna.pietrasik@p.lodz.pl, marketa.ilcikova@savba.sk

Abstract

The specific interactions between polyacrylamide brushes composed of polyacrylamide chains tethered to montmorillonite particles (Mt-*g*-PAm) and the individual components of immiscible ethylene propylene diene modified with sorbic acid (EPDM) and methyl vinyl silicone (MVQ) blends were studied. The effect of various lengths of PAm chains and their grafting density on montmorillonite (Mt) surface was investigated.

It was determined that, due to interactions generated within the system through carboxyl and amide groups the brush particles were selectively located at the EPDM/MVQ interphase and in the EPDM phase. Furthermore, the longer PAm chains resulted in an increase of the glass transition of EPDM, unification of blend morphology, and the reduction of crystallinity of the MVQ phase. Therefore, precisely designed polymer brushes could be considered as novel functional compatibilizers, that provide a new tool for the future material designing.

Keywords: polymer brushes, polyacrylamide, montmorillonite, polymer blends, compatibilizers

Graphical abstract

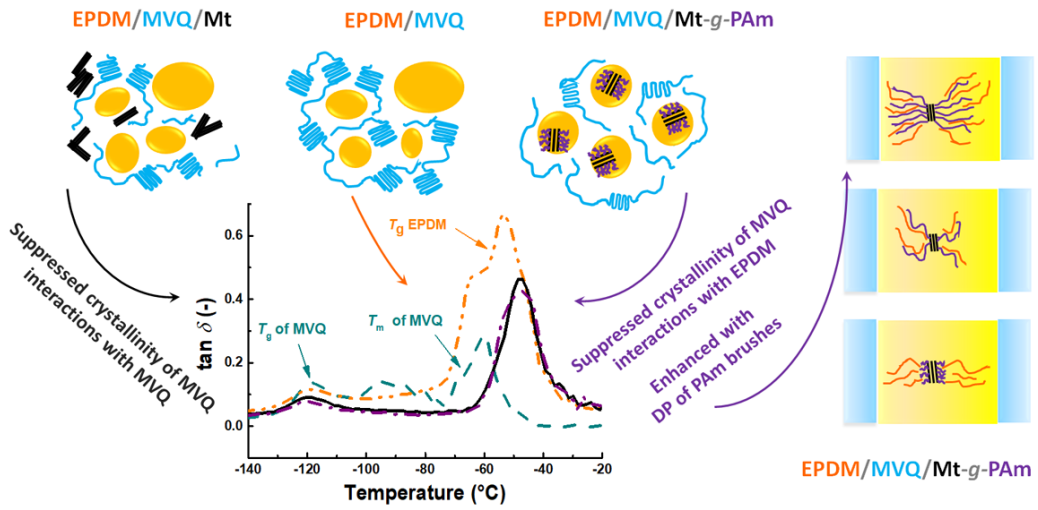

1. Introduction

Hybrid polymer particles are a subject of increasing interest in designing polymer composites. They are formed of organic or inorganic core and polymer shell, which molecular architecture can be tailored by using controlled polymerization techniques [1,2]. The benefits of particle-polymer hybrids are based on the combination of particles properties and interactions of the polymer shell with polymer matrix that allow to control the particle dispersion and location within the matrix. The specific location of particles in well-organized morphologies of block copolymers as well as polymer blends can be obtained by adjusting the suitable polymer shell morphology [3,4]. The advantageous effects on properties of specifically located particles were already described, including compatibilization effect of particles in polymer blends [5–10]. The effect of blend compatibilization is of high interest because the majority of polymers is immiscible, and need to be compatibilized to improve their performance.

In this study the attention is paid to performance of ethylene-propylene-diene terpolymer (EPDM)/methyl vinyl silicone (MVQ) blend. This blend combines superior resistance of

EPDM to oxidation, ozone or weathering ageing and flexibility over a wide temperature range combined with the excellent heat resistance, hydrophobicity and electric properties under wet conditions of silicone rubber [11–13]. In our previous work the significant effect of polymer architecture of clay hybrid particles on damping properties of EPDM/MVQ was revealed. Namely, the effect of length and grafting density of polyacrylamide brushes (PAm) was correlated to mechanical and viscoelastic properties of blend. The PAm chains were grafted from clay particles (Mt) to allow interactions with carboxyl groups on modified EPDM matrix.

Some other approaches of interactions improvement in EPDM/MVQ blend were also reported [14–20]. They are based on either physical interactions, i.e. dipole-dipole interactions, van der Waals forces and hydrogen bonding or chemical interactions *via* covalent bonds formation during reactive compatibilization. In most cases these interactions can be generated by the addition of third components [14–17] or by chemical modification of one of the blend polymer [18–20]. As a result the improvement of thermal stability, the modulus, tensile strength and the swelling resistance of the blend [18], as well as the improved interactions of the filler and blend component were observed [14].

Although the particle polymer hybrids were recognized as promising blend compatibilizers [5,6,8–10] to best of our knowledge, the systematic correlation of the polymer brush architecture with polymer blend dynamic of individual blend components has not been performed yet. Through the polymer brushes length, the level of chains entanglements can be controlled, while the grafting density determines the interactions potential through alignment of the brushes on the particle surface. In our previous work [21], we suggested the crucial role of the interactions generated between polyacrylamide polymer brushes (PAm) grafted on montmorillonite (Mt) surface and ethylene-propylene-

diene terpolymer modified with sorbic acid and methyl vinyl silicone rubber blend (EPDM/MVQ). Herein, based on the same systems, we investigated deeply those interactions with individual blend components. Dynamic mechanical analysis (DMA) and broadband dielectric spectroscopy (BDS) showed impact on glass transition of both EPDM and MVQ phase. The effects on crystallinity of MVQ phase were studied by XRD. The findings were correlated with polymer blend morphology and particle location. The results showed the chemical nature of the brushes controls the particle location in blend, while architecture affects the dynamics of the polymer matrix. The long brushes suppressed the movement of the compatible blend component thank to entanglements, while on the other hand the short dense brushes facilitated the movement of the polymer matrix chains.

The results presented in this study show that the precise identification and justification of the interactions generated within the blends can serve as a tool for the detailed design of functional compatibilizers as well as control of the blends' properties.

2. Experimental part

2.1 Materials

Methyl vinyl silicone rubber (MVQ, POLYMER MV 007) containing 0.05-0.09 mol% of vinyl units and Mooney viscosity of ML(1+4, 100˚C) = 15 was received from Silikony Polskie Chemical Company (Poland). Ethylene propylene diene terpolymer (EPDM) Keltan 4450S (LANXESS GmbH, Germany) with ethylene content of 42 wt.%, norbornene (NRB) content of 4.3 wt% and Mooney viscosity of ML(1+4, 125˚C) = 44. EPDM was modified with sorbic acid (Sigma Aldrich, USA) as previously reported [21]. Sodium montmorillonite clay AB134225 (Mt-Na) and 3-aminopropylmethyldiethoxysilane (APMDES) of purity 97% were ordered from ABCR

GmbH & Co. KG (Germany). Acrylamide (Am, ≥ 98%), α-bromoisobutyryl bromide (BIBB, 98%), ethyl α-bromoisobutyrate (EBIB, 98%), copper (I) chloride (CuCl, ≥ 99%), 4-(dimethyl)aminopyridine (DMAP ≥ 98,0%), copper (II) chloride ($CuCl_2$, ≥ 99.999%), tris[2-(dimethylamino)ethyl]amine (Me_6TREN, 97%), triethylamine (TEA, ≥ 99%), were purchased from Sigma Aldrich (USA). *Bis*(*α*,*α*-dimethylbenzyl) peroxide (DCP) with purity ≥ 98%) was provided by Merck KGaA (Germany). All reagents were used as received, except Am. Am was purified in order to remove the inhibitor according to a previously reported procedure [21]. Solvents: methanol (99.8%), ethanol (96%), acetone (99.5%), dichloromethane (99.8%) and toluene (99.5%), were purchased from POCH S.A (Poland). In order to remove residual water from toluene, it was refluxed over sodium under an inert atmosphere and subsequently vacuum distilled. All other solvents were used as received.

2.2 Preparation of Mt-g-PAm hybrids

The montmorillonite-*g*-polyacrylamide (Mt-*g*-PAm) hybrids, as well as EPDM/MVQ blends, were prepared according to previously described procedures [21]. Briefly, Mt-Na was initially acid-activated, silanized and then functionalized with atom transfer radical polymerization (ATRP) initiators. Then surface – initiated ATRP of acrylamide was performed. Three montmorillonite-*graft*-polyacrylamide hybrids particles (Mt-*g*-PAm: Mt1, Mt2 and Mt3) were obtained with varied PAm chain length and grafting densities.

2.3 Preparation of blends

EPDM-COOH/MVQ rubber mixtures containing different Mt-*g*-PAm hybrids, unmodified montmorillonite (Mt-Na) and unmodified Mt-Na mixed with linear polyacrylamide (PAm) were prepared in a Brabender Measuring Mixer N50 micromixer (Brabender GmbH & Co. KG, Germany) and then vulcanized in a sheet format using a

hydraulic press, according to the procedure described previously [21]. A neat blend without Mt-*g*-PAm particles was also prepared. All blends contained 50 phr of EPDM-COOH, 50 phr of MVQ, 2.5 phr of DCP and additionally: 3 phr of Mt-Na, (EPDM/MVQ/Mt); 1.1 phr of Mt-Na and 1.9 phr of PAm (EPDM/MVQ/Mt+PAm); 3 phr of Mt1, Mt2 and Mt3 (EPDM/MVQ/Mt1, EPDM/MVQ/Mt2 and EPDM/MVQ/Mt3, respectively). A neat blend without filler was also prepared as a reference sample and assigned as EPDM/MVQ.

2.3 Characterization techniques

The molecular weight of PAm was determined using gel permeation chromatography (GPC). The reported EPDM/MVQ blends and their composites were characterized by dynamic mechanical analysis (DMA) in tensile mode, melt rheology in shear mode, X-ray diffraction (XRD), scanning electron microscopy (SEM) and broadband dielectric spectroscopy (BDS). The detailed methodology is described in SI.

3. Results and discussion

3.1. Mt-*g*-PAm characterization

The PAm synthesized from Mt surface, Mt-*g*-PAm, was characterized by GPC. However, it appeared the cleavage of PAm from Mt particles was not successful, due to the possible hydrolysis of PAm by hydrofluoric acid, which can occur at low pH [22]. Therefore, assuming the similar molar mass of brushes grown from the surface and from sacrificial initiator [23, 24] PAm synthesized in solution, using ethyl bromoisobutyrate as initiator, was analyzed and the GPC traces of the free PAm were collected (Fig. S1). In a case of monomer to initiator ratio equaled 600:1, the M_n was 18 400 g mol^{-1} and $Đ$ =1.41 (Mt2), while for 3000:1, M_n was 45 000 g mol^{-1} and Đ= 1.49, (Mt3). These results were obtained for systems containing particles with higher concentration of initiator immobilized on Mt

surface, (0.5469 mmol g^{-1}). If the polymerization was performed in presence of Mt particles with lower initiator concentration (0.0594 mmol g^{-1}), PAm with Mn=55 300 g mol^{-1} and Đ=1.46, (Mt1) was obtained; chromatogram was not shown.

The molecular weight of free polymers obtained for each system was used together with the results of thermogravimetric analysis (TGA), described previously [21], to calculate the grafting densities of all hybrids [23]. For Mt1 it was calculated to be σ = 0.008 chains nm^{-2}, for Mt2: σ = 0.028 chains nm^{-2} and for Mt3: σ = 0.014 chains nm^{-2}. Therefore, it was concluded the obtained hybrids varied with both, molecular weight and grafting density of tethered on Mt surface PAm chains.

3.2. Viscoelastic properties

The effect of filler modification on the viscoelastic properties of EPDM/MVQ polymer blends was studied by DMA in tensile mode. In the Fig. 1a, three characteristic transitions can be observed in temperature dependence of storage modulus (*E*'), i.e. the glass transition of MVQ, melting of MVQ crystalline phase, and glass transition of EPDM, at ~ -120 °C, -60 °C and -50 °C, respectively. The effects of filler addition and surface modification is most evident in tan δ temperature dependence, Fig. 1b. The inset in Fig. 1b magnifies the glass transition (T_g) of MVQ phase. The addition of Mt reduced the peak height, while the effect was more pronounced by using modified Mt-*g*-PAm. The decrease of peak height indicates restriction of MVQ segmental motion due to enhanced interactions between Mt-*g*-PAm and EPDM/MVQ, thanks to presence of PAm. On the other hand, the T_g of EPDM was significantly affected, the peak maximum was shifted from -53.7 °C to -46.6 °C, for EPDM/MVQ and EPDM/MVQ/Mt composites, respectively. This points to enhanced interactions of Mt and Mt-*g*-PAm with the EPDM phase.

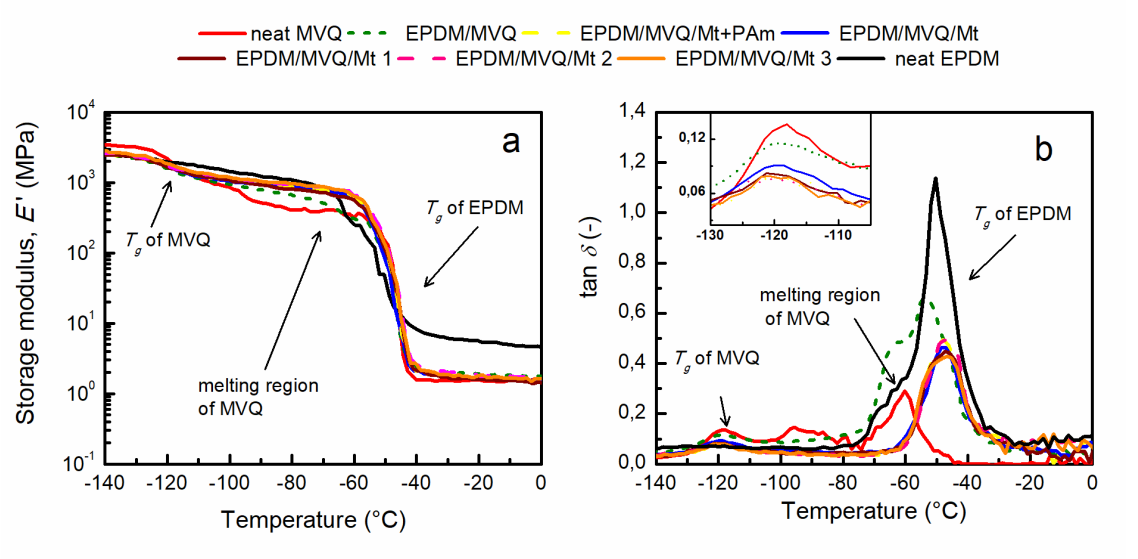

Fig. 1. Temperature dependence of (a) the storage modulus (*E*') and (b) tan δ measured in tensile mode of EPDM/MVQ blends and its composites.

The EPDM glass transition was studied by two methods, in tensile mode by DMA and in shear mode by rotational rheometer, due to better accuracy of the rheometer in this temperature range. Although the absolute values differ, the trends are similar to those obtained from DMA measurements. To quantify the effect of the Mt and Mt-*g*-PAm hybrids on the segmental dynamics, the pseudoactivation energies (E_a) of EPDM glass transition were calculated based on the Arrhenius theory using a modified equation (1), [25, 26]:

$$\ln f = \ln f_0 - \frac{E_a}{RT_g} \quad (1)$$

where f is the tested frequency, f_0 represents the characteristic constant of the material, T_g is the glass transition temperature, and R is the universal gas constant.

The results are summarized in Table 1.

When focused on E_a determined from DMA in tensile mode, the highest E_a was observed in the system with long PAm grafts: Mt1(M_n = 55 300 g mol^{-1}, σ = 0.008 chains nm^{-2}) and Mt3 (M_n = 45 000 g mol^{-1}, σ = 0.014 chains nm^{-2}), i.e. loosely and densely arranged chains, and the values reached 80.9 and 82.0 kJ mol^{-1}, respectively. Compared to E_a of EPDM/MVQ, the energy barrier increased by 23 % and 24 %. Regardless of the grafting density, the longer chains of M_n = 55 300 g mol^{-1} and M_n = 45 000 g mol^{-1} effectively interacted with EPDM, compared to short graft chains (M_n = 18 400 g mol^{-1}) in the Mt2 system. The E_a of MVQ phase decreased with filler addition. These results are consistent with crystallinity content observed in Fig. 1b. While the crystalline phase is easily detected in EPDM/MVQ blends, the peak disappeared completely in the composites. Interestingly, the E_a of MVQ increased in EPDM blends, which may point to EPDM as the nucleation agent for the MVQ phase. The effects of the filler addition on the crystalline phase of MVQ was studied by XRD.

Table 1 The pseudoactivation energies E_a for neat EPDM and MVQ as well as EPDM/MVQ blends and composites. E_a calculated from dynamic mechanical analyzer in tensile mode and rotational rheometer in shear mode.

Sample name	**Tensile mode**		**Shear mode**
	E_a α for MVQ (kJ mol^{-1})	**E_a α for EPDM (kJ mol^{-1})**	**E_a α for EPDM glass transition (kJ mol^{-1})**
MVQ	5.86	ND*	ND*
EPDM	ND*	66.2	101.0
EPDM/MVQ	6.49	65.9	101.0
EPDM/MVQ/Mt+PAm	4.47	61.4	97.9
EPDM/MVQ/Mt	4.53	73.2	103.2
EPDM/MVQ/Mt1	4.66	80.9	119.1
EPDM/MVQ/Mt2	4.45	75.1	108.0
EPDM/MVQ/Mt3	4.61	82.0	122.6

**ND – not detectable*

3.3 Crystallinity of MVQ blend component studied by XRD

Fig. 2 shows the spectra for the neat MVQ, Mt, and EPDM/MVQ composites. The crystalline peak of MVQ is clearly seen at 14.8°. In the blend with EPDM the MVQ crystallinity peak, observed by DMA, increased which proved the nucleating agent effect of EPDM. The addition of Mt and Mt-*g*-PAm suppressed the crystallinity of MVQ. The effect is most pronounced in the case of long and densely grafted PAm chains, Mt3 (M_n = 45 000 g mol^{-1}, σ = 0.014 chains nm^{-2}), where the shift of peak maxima to a lower 2θ was observed. The shift is related to the increased space between lamellas of MVQ crystalline phase, where the light is scattered. As a result, the MVQ phase is less concise. This observation can be the consequence of development of a finer morphology, i.e. EPDM domains are smaller and prevent MVQ phase from organization and formation of well-ordered crystal domains.

Additionally, the presence of peaks at 7.5° and 23.2° should be noted. They originate from layers of Mt, [27,28] and are not evident either in system containing neat Mt+PAm or Mt-*g*-PAm hybrid composites. This observation confirms the intercalation and exfoliation of Mt with PAm.

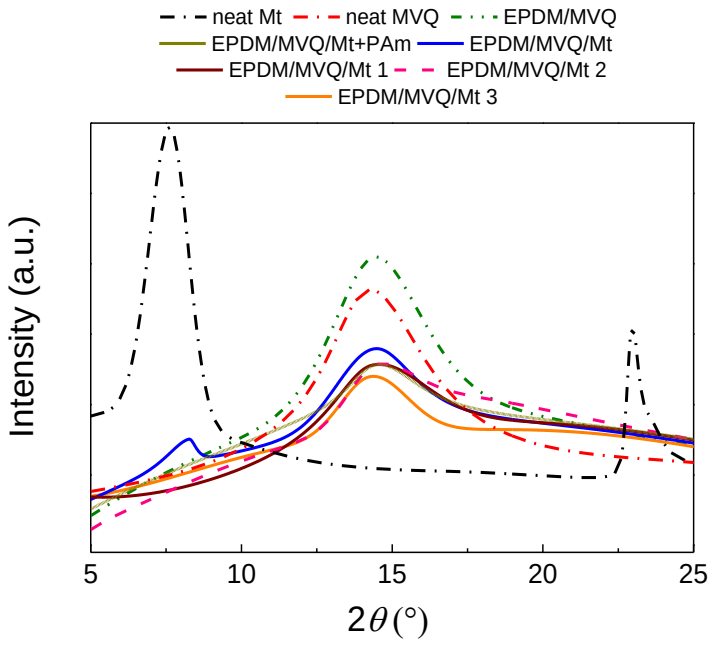

Fig. 2. XRD pattern of the neat MVQ, neat Mt as well as EPDM/MVQ blend and composites.

3.4 Morphology of EPDM/MVQ blends

The morphology of the blends was investigated using SEM/SE and SEM/BSE imaging. Figure 3 shows the SEM/BSE micrographs of the EPDM/MVQ/Mt composite, the blend with neat Mt+PAm, and the blend composites with Mt2 and Mt3, (M_n = 18 400 g mol^{-1}, σ = 0.028 chains nm^{-2}and M_n = 45 000 g mol^{-1}, σ = 0.014 chains nm^{-2}), respectively. The complete set of SEM micrographs of all investigated samples are shown in Fig. S2. In SEM/BSE micrographs (Fig. 3) the contrast increases with average atomic number of given phase. Therefore, the brighter phase corresponds to MVQ, while the darker phase shows EPDM, and the brightest areas (spots) correspond to clay particles and/or agglomerates. The blend components were arranged into “sea-island” morphology, in which the EPDM droplets were dispersed in MVQ phase. The neat Mt as well as Mt

mixed with free dispersed PAm occured in MVQ phase, as documented in Fig. 3a and Fig. 3b. Analysis of the dispersion of these two samples revealed a non-uniform distribution of the filler particles and the presence of agglomerates.

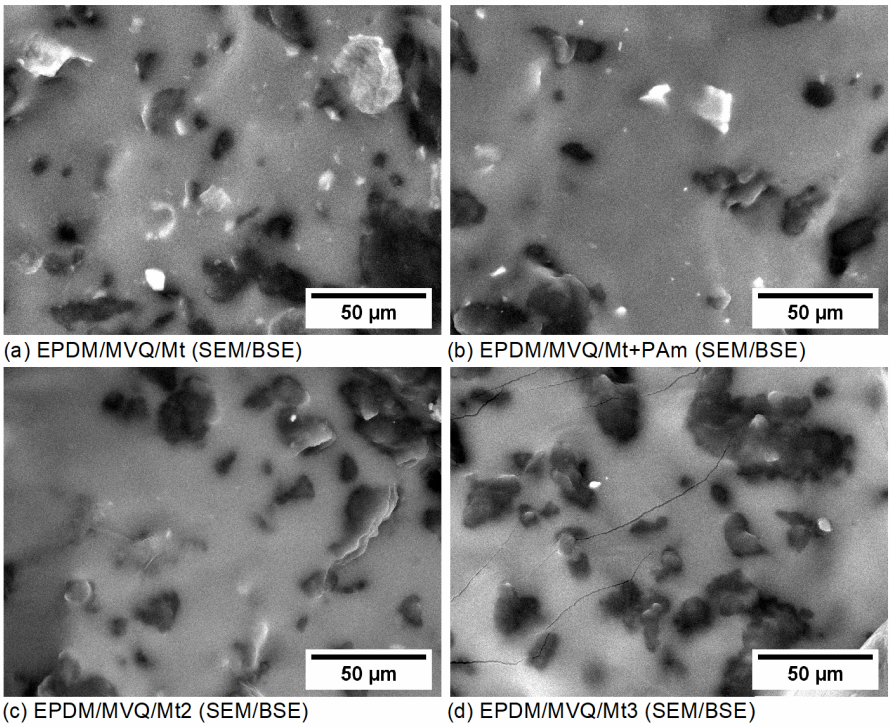

(a) EPDM/MVQ/Mt (SEM/BSE) (b) EPDM/MVQ/Mt+PAm (SEM/BSE)

(c) EPDM/MVQ/Mt2 (SEM/BSE) (d) EPDM/MVQ/Mt3 (SEM/BSE)

Fig. 3. SEM/BSE images of EPDM/MVQ blends containing Mt, Mt+PAm and Mt-*g*-PAm: Mt2 and Mt3.

The location of the neat Mt in the MVQ phase could be predicted also from calculations of the wetting coefficient. It was concluded that PAm is more compatible with EPDM phase, thus the location of Mt-*g*-PAm hybrids in the EPDM or at the interphase is consistent with the previous findings [21]

SEM/BSE micrographs also revealed the more uniform dispersion of particles and the slightly smaller size of the aggregates for both hybrids with higher grafting density Mt2 and Mt3, Fig. 3c and Fig. 3d, M_n = 18 400 g mol^{-1}, σ = 0.028 chains nm^{-2} and M_n = 45 000 g mol^{-1}, σ = 0.014 chains nm^{-2}, respectively. This could result from the higher local

concentration of functional amide groups that were able to interact with the carboxylic groups of functionalized EPDM.

The effects of Mt and Mt-*g*-PAm on particle location, crystallinity of MVQ phase and blends morphology are illustrated schematically in Fig. 4.

The interactions of EPDM with PAm chains were further investigated by broadband dielectric spectroscopy. That allows to study the segmental as well as side chain groups relaxations over a broad temperature and frequency range.

Fig. 4. The illustration of the effect of Mt and Mt-*g*-PAm presence in the blends on morphology and crystallinity of MVQ phase and particle location.

3.5. EPDM/MVQ and Mt-*g*-PAm interactions

The three relaxation processes were found in the EPDM/MVQ blends. The segmental motions (α relaxations) attributed to T_g of both MVQ and EPDM components, as well as side chain (*β* relaxations) of -COOH groups of modified EPDM were recognized. The possible interactions of amide groups present in PAm and with -COOH groups tethered on EPDM chains are summarized in Fig. 5. Dipole-dipole interactions and hydrogen bonding were expected to occur, affecting the dielectric response.

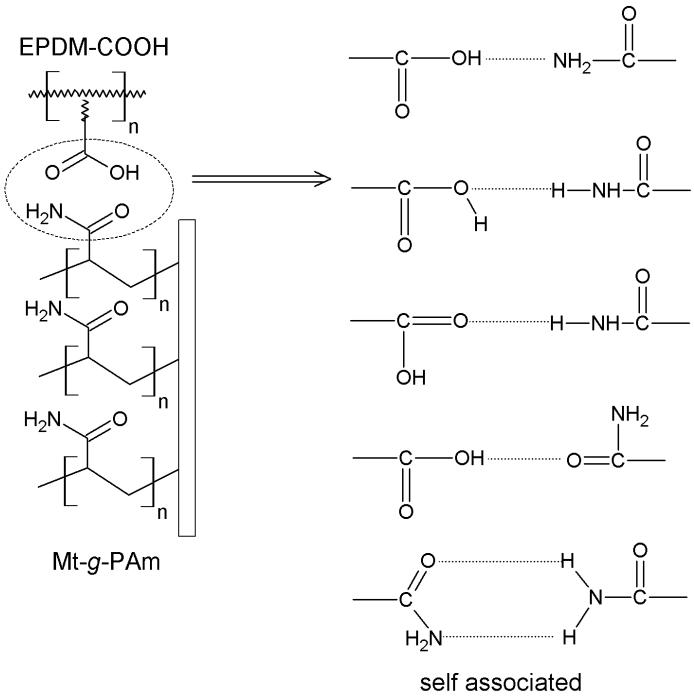

Fig. 5. Possible interactions between EPDM modified with carboxylic groups and amide groups of polyacrylamide chains attached to Mt, Mt-*g*-PAm hybrids.

The evaluation of the effects of the filler on the relaxations was performed through calculation of the activation energies of the relaxation processes according to the equations (2) and (3). The E_a of the main relaxations (α and Maxwell-Wagner-Sillars (MWS)) were quantified based on the Vogel-Fulcher-Tamman equation (3) in a similar manner as for various polymeric [29], elastomeric [30] or composite [31] systems.

$$f = f_0 \exp\left(\frac{E_a}{k(T - T_0)}\right) \quad (2)$$

where, f is the relaxation frequency, f_0 is the pre-exponential factor, E_a is the activation energy, T is the thermodynamic temperature, T_0 is Vogel temperature, and k is the Boltzmann's constant.

The β relaxation processes, such as side groups relaxation or other processes, were evaluated and the E_a were calculated according to Arrhenius equation (3).

$$f_\beta = f_\infty \exp\left(\frac{E_a}{k_B T}\right) \quad (3)$$

where E_a is the activation energy, f_∞ is the pre-exponential factor, T is thermodynamic temperature, and k_B is Boltzmann constant.

The non-linear behavior, which results mainly from α-relaxations, was fit with a VFT model, while the linear behavior was fit using the Arrhenius model. The calculated results of E_a are compiled in Table 2 and Fig. 6. The complete list of fit parameters of both Arrhenius and VFT model are listed in Table S1. The 3D plots of dielectric moduli as a function of temperature and frequency for all samples are shown in SI, Fig. S3.

Table 2 Activation energies of glass transitions and β relaxation process of COOH attached on EPDM, the data calculated on VFT and Arrhenius models.

Sample name	**VFT α-relaxation MVQ**	**VFT α-relaxation EPDM**	**Arrhenius β-relaxation - COOH**
	B (kJ mol^{-1})	**B (kJ mol^{-1})**	**E_a (kJ mol-^{1})**
MVQ	5.5	ND*	ND*
EPDM	ND*	10.2	49.7
EPDM/MVQ	6.8	10.6	ND*
EPDM/MVQ/Mt+PAm	4.3	10.3	ND*
EPDM/MVQ/Mt	4.5	10.7	ND*
EPDM/MVQ/Mt1	4.7	11.4	51.0
EPDM/MVQ/Mt2	4.6	9.0	ND*
EPDM/MVQ/Mt3	4.6	11.9	54.6

**ND – not detectable*

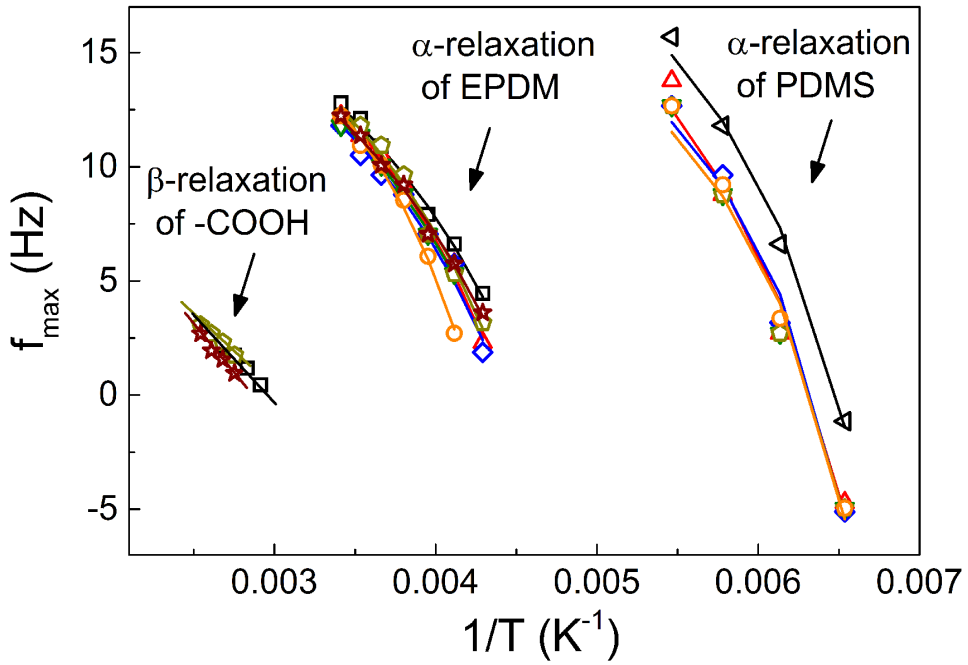

Fig. 6. Dielectric map for various samples and corresponding plots (VFT, Arrhenius), where EPDM/MVQ is red triangles, EPDM/MVQ/Mt is green down triangles, EPDM/MVQ/Mt+PAm is blue diamonds, EPDM/MVQ/Mt1 is dark yellow pentacle, EPDM/MVQ/Mt2 is orange circles and EPDM/MVQ/Mt3 is wine stars.

The presence of Mt mostly affected the α relaxation of MVQ phase. Compared to neat EPDM/MVQ blend the values of E_a of MVQ α relaxation decreased significantly after filler addition. In other words, the presence of particles decreased the energy barrier needed for relaxation that facilitates the MVQ dipoles to interact with external electric field. That is because Mt was preferentially located in MVQ while Mt-*g*-PAm hybrids at the interphase and did not provide any specific interactions with MVQ phase.

Additionally, in case of blends containing PAm brushes with higher molecular weight (Mt1 and Mt3 hybrids) the effects on both α and β relaxations of EPDM are visible. The α relaxation increased from 10.2 kJ mol^{-1} for neat blend EPDM/MVQ to 11.4 kJ mol^{-1}

and 11.9 kJ mol^{-1} for blends enriched with Mt-*g*-PAm hybrids with long PAm chains, regarding the polymer grafting densities; 0.008 chains nm^{-2} (Mt1) and 0.014 chains nm^{-2} (Mt3), respectively. The value of βE_a was also higher in comparison to neat EPDM. That means that the long PAm brushes enable the Mt-*g*-PAm hybrids to interact with EPDM phase. Those results follow SEM observations, showing PAm grafted particles were found at the interphase, and also correlate with dynamic mechanical analysis data.

Conclusions

The specific interactions between Mt-*g*-PAm hybrids and individual components of EPDM/MVQ blend were elucidated in this article. In order to induce those interactions, EPDM was modified with COOH groups, while PAm chains immobilized on Mt surface were varied by their length and grafting density. Due to the nature of carboxyl and amide groups dipole-dipole interactions and hydrogen bonding were formed. SEM revealed better dispersion and distribution of Mt-*g*-PAm in the EPDM/MVQ, finer morphology and improved homogeneity of the blend. The Mt-*g*-PAm were rather observed in EPDM phase or at the interface. The preferred location in EPDM phase was supported by DMA as well as BDS measurements. The viscoelastic measurements showed the activation energy of EPDM glass transition was enhanced by 23 % and 24 % in case of long and loose (M_n = 55 300 g mol, σ = 0.008 chains nm^{-2}) and dense (M_n = 45 000 g mol^{-1}, σ = 0.014 chains nm^{-2}) grafts, respectively. That revealed the long chains are most effective in formation of interactions with EPDM phase.

It was demonstrated that both the chemical character of blend components as well as precisely designed architecture of novel hybrid compatibilizers can provide a good tool

for tailoring material properties. Such approach opens new perspectives for composite materials design based on polymer blends and polymer brushes particles.

Acknowledgement

The authors thank to National Science Centre, Poland for the financial support through POLONEZ (UMO-2016/23/P/ST5/02131) which has received funding from the European Unions's Horizon 2020 research and innovation program under Marie Sklodowska-Curie grant agreement. No 665778. This work was supported by the Ministry of Education, Youth and Sports of the Czech republic - DKRVO (RP/CPS/2020/003). This study was also performed during the implementation of the project Building-up Centre for advanced materials application of the Slovak Academy of Sciences, ITMS project code 313021T081 supported by Research & Innovation Operational Programme funded by the ERDF. JM acknowledges for financial support to project VEGA 2/0129/19. MI and JM acknowledge APVV-19-0338.

Conflicts of Interest: The authors declare no conflict of interest.

Author contributions

Monika Galeziewska: Investigation, Formal analysis, Writing – original draft; Magdalena Lipinska: Conceptualization, Investigation, Formal analysis, Writing – original draft; Miroslav Mrlik: Methodology, Data curation, Formal analysis; Marketa Ilcikova: Methodology, Formal analysis, Writing – original draft; Miroslav Slouf: Methodology, Formal analysis; Veronika Gajdosova: Investigation; Eva Achbergerová: Methodology; Lenka Musilová: Methodology; Jaroslav Mosnacek: Writing –original draft; Joanna Pietrasik: Conceptualization, Supervision, Writing – original draft

References

[1] J. Yan, M.R. Bockstaller, K. Matyjaszewski, Brush-modified materials: Control of molecular architecture, assembly behavior, properties and applications, Prog. Polym. Sci. 100 (2020) 101180. https://doi.org/10.1016/j.progpolymsci.2019.101180.

[2] C.M. Hui, J. Pietrasik, M. Schmitt, C. Mahoney, J. Choi, M.R. Bockstaller, K. Matyjaszewski, Surface-Initiated Polymerization as an Enabling Tool for Multifunctional (Nano-)Engineered Hybrid Materials, Chem. Mater. 26 (2014) 745–762. https://doi.org/10.1021/cm4023634.

[3] M. Salzano De Luna, G. Filippone, Effects of nanoparticles on the morphology of immiscible polymer blends - Challenges and opportunities, Eur. Polym. J. 79 (2016) 198–218. https://doi.org/10.1016/j.eurpolymj.2016.02.023.

[4] A. Taguet, P. Cassagnau, J.M. Lopez-Cuesta, Structuration, selective dispersion and compatibilizing effect of (nano)fillers in polymer blends, Prog. Polym. Sci. 39 (2014) 1526–1563. https://doi.org/10.1016/j.progpolymsci.2014.04.002.

[5] Y. Cao, J. Feng, P. Wu, Polypropylene-grafted graphene oxide sheets as multifunctional compatibilizers for polyolefin-based polymer blends, J. Mater. Chem. 22 (2012) 14997–15005. https://doi.org/10.1039/c2jm31477k.

[6] B. Du, U.A. Handge, M. Wambach, C. Abetz, S. Rangou, V. Abetz, Functionalization of MWCNT with P(MMA-co-S) copolymers via ATRP: Influence on localization of MWCNT in SAN/PPE 40/60 blends and on rheological and dielectric properties of the composites, Polymer (Guildf). 54 (2013) 6165–6176. https://doi.org/10.1016/j.polymer.2013.08.065.

[7] L. Elias, F. Fenouillot, J.C. Majesté, P. Alcouffe, P. Cassagnau, Immiscible

polymer blends stabilized with nano-silica particles: Rheology and effective interfacial tension, Polymer (Guildf). 49 (2008) 4378–4385. https://doi.org/10.1016/j.polymer.2008.07.018.

[8] Z. Fu, H. Wang, X. Zhao, S. Horiuchi, Y. Li, Immiscible polymer blends compatibilized with reactive hybrid nanoparticles: Morphologies and properties, Polymer (Guildf). 132 (2017) 353–361. https://doi.org/10.1016/j.polymer.2017.11.004.

[9] D. Han, T. jiao Wen, G. Han, Y. yi Deng, Y. Deng, Q. Zhang, Q. Fu, Synthesis of Janus POSS star polymer and exploring its compatibilization behavior for PLLA/PCL polymer blends, Polymer (Guildf). 136 (2018) 84–91. https://doi.org/10.1016/j.polymer.2017.12.050.

[10] T. Parpaite, B. Otazaghine, A.S. Caro, A. Taguet, R. Sonnier, J.M. Lopez-Cuesta, Janus hybrid silica/polymer nanoparticles as effective compatibilizing agents for polystyrene/polyamide-6 melted blends, Polymer (Guildf). 90 (2016) 34–44. https://doi.org/10.1016/j.polymer.2016.02.044.

[11] H. Acharya, S. Kumar Srivastava, EPDM/silicone blend layered silicate nanocomposite by solution intercalation method: Morphology and properties, Polym. Compos. 35 (2014) 1834–1841. https://doi.org/10.1002/pc.22848.

[12] M. Ehsani, H. Borsi, E. Gockenbach, J. Morshedian, G.R. Bakhshandeh, An investigation of dynamic mechanical, thermal, and electrical properties of housing materials for outdoor polymeric insulators, Eur. Polym. J. 40 (2004) 2495–2503. https://doi.org/10.1016/j.eurpolymj.2004.03.014.

[13] R. Deepalaxmi, V. Rajini, C. Vaithilingam, S. Vijayalakshmi, Analysis of Gamma Irradiation Effects on Dielectric Parameters, J. Eng. Sci. Technol. 14

(2019) 1118–1137.

[14] L. Bazli, A. Khavandi, M.A. Boutorabi, M. Karrabi, Correlation between viscoelastic behavior and morphology of nanocomposites based on SR/EPDM blends compatibilized by maleic anhydride, Polymer (Guildf). 113 (2017) 156–166. https://doi.org/10.1016/j.polymer.2017.02.057.

[15] W. Zhang, W. Yan, R. Pan, W. Guo, G. Wu, Synthesis of silane-grafted ethylene vinyl acetate copolymer and its application to compatibilize the blend of ethylene-propylene-diene copolymer and silicone rubber, Polym. Eng. Sci. 58 (2018) 719–728. https://doi.org/10.1002/pen.24604.

[16] C. Zhang, Z.X. Zhang, K. Pal, O.G. Shin, H. Choel Jo, S.H. Lee, J.K. Kim, Effect of Silanes on Mechanical and Thermal Properties of Silicone Rubber/EPDM Blends, J. Macromol. Sci. Part B. 50 (2010) 291–299. https://doi.org/10.1080/00222341003651494.

[17] S. Kole, R. Santra, A.K. Bhowmick, Studies of in-situ compatibilized blend of silicone and EPDM rubbers, Rubber Chem. Technol. 67 (1994) 119–128. https://doi.org/10.5254/1.3538658.

[18] S. Kole, S. Roy, A.K. Bhowmick, Influence of chemical interaction on the properties of silicone-EPDM rubber blend, Polymer (Guildf). 36 (1995) 3273–3277. https://doi.org/10.1016/0032-3861(95)99425-T.

[19] J. Konar, S. Kole, B.N. Avasthi, A.K. Bhowmick, Wetting behavior of functionalized silicone and EPDM rubber, J. Appl. Polym. Sci. 61 (1996) 501–506. https://doi.org/10.1002/(SICI)1097-4628(19960718)61:3<501::AID-APP13>3.0.CO;2-3.

[20] S. Kole, S. Roy, A.K. Bhowmick, Interaction between silicone and EPDM

rubbers through functionalization and its effect on properties of the blend, Polymer (Guildf). 35 (1994) 3423–3426. https://doi.org/10.1016/0032-3861(94)90904-0.

[21] M. Zygo, M. Lipinska, Z. Lu, M. Ilcíková, M.R. Bockstaller, J. Mosnacek, J. Pietrasik, New type of montmorillonite compatibilizers and their influence on viscoelastic properties of ethylene propylene diene and methyl vinyl silicone rubbers blends, Appl. Clay Sci. 183 (2019) 105359. https://doi.org/10.1016/j.clay.2019.105359.

[22] M.J. Caulfield, G.G. Qiao GG, D.H. Solomon, Some aspects of the properties and degradation of polyacrylamides, Chem. Rev. 102 (2002) 3067-3084. https://doi.org/10.1021/cr010439p.

[23] M. Ilcikova, M. Galeziewska, M. Mrlik, J. Osicka, M. Masar, M. Slouf, M. Maslowski, M. Kracalik, R. Pietrasik, J. Mosnacek, J. Pietrasik, The effect of short polystyrene brushes grafted from graphene oxide on the behavior of miscible PMMA/SAN blends, Polymer 211 (2011) 123088. htps://doi.org/10.1016/j.polymer.2020.123088

[24] K. Ohno, T. Morinaga, K. Koh, Y. Tsujii, T. Fukuda, Synthesis of monodisperse silica particles coated with well-defined, high-density polymer brushes by surface-initiated atom transfer radical polymerization, Macromolecules 38 (2005) 2137-2142. https://doi.org/10.1021/ma048011q

[25] M. Ilčíková, M. Mrlík, T. Sedláček, M. Šlouf, A. Zhigunov, K. Koynov, J. Mosnáček, Synthesis of Photoactuating Acrylic Thermoplastic Elastomers Containing Diblock Copolymer-Grafted Carbon Nanotubes, ACS Macro Lett. 3 (2014) 999–1003. https://doi.org/10.1021/mz500444m.

[26] M. Cvek, M. Mrlík, M. Ilčíková, J. Mosnáček, L. Münster, V. Pavlínek, Synthesis of Silicone Elastomers Containing Silyl-Based Polymer-Grafted Carbonyl Iron Particles: An Efficient Way To Improve Magnetorheological, Damping, and Sensing Performances, Macromolecules. 50 (2017) 2189–2200. https://doi.org/10.1021/acs.macromol.6b02041.

[27] E.S. Kim, E.J. Kim, T.H. Lee, J.S. Yoon, Improvement of the adhesion properties of silicone rubber by the incorporation of silane-modified montmorillonite, J. Appl. Polym. Sci. 128 (2013) 2563–2570. https://doi.org/10.1002/app.38489.

[28] N.I.N. Ismail, A. Ansarifar, M. Song, Preparation and characterization of high performance exfoliated montmorillonite/silicone rubber nanocomposites with enhanced mechanical properties, Polym. Eng. Sci. 53 (2013) 2603–2614. https://doi.org/10.1002/pen.23528.

[29] M. Füllbrandt, S. Wellert, R. von Klitzing, A. Schönhals, Thermal and corrosion (in)stability of polyamide 6 studied by broadband dielectric spectroscopy, Polymer (Guildf). 75 (2015) 34–43. https://doi.org/10.1016/J.POLYMER.2015.08.016.

[30] G.D. Smith, D. Bedrov, Relationship between the α- and β-relaxation processes in amorphous polymers: Insight from atomistic molecular dynamics simulations of 1,4-polybutadiene melts and blends, J. Polym. Sci. Part B Polym. Phys. 45 (2007) 623–643. https://doi.org/10.1002/polb.21064.

[31] J. Zhang, M. Mine, D. Zhu, M. Matsuo, Electrical and dielectric behaviors and their origins in the three-dimensional polyvinyl alcohol/MWCNT composites with low percolation threshold, Carbon N. Y. 47 (2009) 1311–1320. https://doi.org/10.1016/J.CARBON.2009.01.014.

Supplementary information

Polyacrylamide brushes with varied morphologies as a tool for control of the intermolecular interactions within EPDM/MVQ blends

Monika Galeziewska[1], Magdalena Lipinska[1], Miroslav Mrlik[2], Marketa Ilcikova[1,3*], Veronika Gajdosova[4], Miroslav Slouf[4], Eva Achbergerová[5], Lenka Musilová[6], Jaroslav Mosnacek[3,7], Joanna Pietrasik[1*]

[1] Lodz University of Technology, Department of Chemistry, Institute of Polymer and Dye Technology, Stefanowskiego 12/16, 90 924 Lodz, Poland

[2] Tomas Bata University in Zlin, University Institute, Centre of Polymer Systems, Trida T. Bati 5678, Zlin 76001, Czech Republic

[3] Polymer Institute, Slovak Academy of Sciences, Dubravska cesta 9, 845 41 Bratislava, Slovakia

[4] Institute of Macromolecular Chemistry, Czech Academy of Sciences, Heyrovskeho namesti 2, 162 06 Praha 6, Czech Republic

[5] CEBIA-Tech, Faculty of Applied Informatics, Tomas Bata University in Zlín, Nad Stráněmi 4511, 760 05 Zlín, Czech Republic

[6] Department of Physics and Materials Engineering, Faculty of Technology, Tomas Bata University in Zlin, Vavrečkova 5569, 760 01 Zlín, Czech Republic

[7] Centre for Advanced Materials Application, Slovak Academy of Sciences, Dubravska cesta 9, 845 11 Bratislava, Slovakia

1. Methods

1.1 Gel permeation chromatography

1.2 Dynamic mechanical analysis

The viscoelastic properties of all nanocomposites were measured in both tensile and shear mode. The tensile mode was applied for dynamic mechanical analysis (DMA) using rectangular shape samples with the following dimensions; length 10 mm, width 1.9 mm and thickness 0.32 mm. All measurements were performed at the linear viscoelastic region (7 μm deformation was used), at selected frequencies (0.5, 1, 2.5 and 5 Hz) at temperature range from -150°C to 150°C using a DMA 1 (Mettler Toledo, Switzerland) apparatus. The shear mode was measured in a rotational oscillation rheometer, Ares G2 (TA Instruments, USA) equipped with parallel-plate geometry (diameter of 25 mm). The measurements of storage shear modulus, $G^{'}$, and loss shear modulus $G^{''}$, were carried out as a function of temperature. The temperature sweep tests were carried out with a heating rate of 2°C min^{-1} at constant angular frequency of 0.5, 1.5, 5, 10 Hz and at oscillation strain of 0.02%, over a temperature range from -10°C to -70°C. Circular shape samples with diameter of 25 mm and thickness of 0.8 mm were used.

1.3 Dielectric properties

The dielectric properties were investigated using a Broadband Dielectric Impedance Analyzer (Novocontrol, Germany) equipped with standard sample cell BDCS 140. The measurements were conducted in the frequency range from 0.1 Hz to 10 MHz and over a temperature range from -150°C to 150°C. The permittivity was recalculated to dielectric moduli using the equations (1) [1,2]:

$$M^* = \frac{1}{\varepsilon^*}$$
$$M' = \frac{\varepsilon'}{\varepsilon'^2 + \varepsilon''^2}$$
$$M'' = \frac{\varepsilon''}{\varepsilon'^2 + \varepsilon''^2} \quad (1)$$

where, ε^* is complex permittivity, ε' and ε'' are relative permittivity and loss permittivity, respectively. M^*, M' and M'' are complex, storage and loss dielectric moduli, respectively. The application of equations (1) is necessary for conducting samples or samples where electrode polarization is very strong, similar to what was observed in other cases [2].

1.4 X-ray diffraction

Crystalline phase of the neat Mt and EPDM/MVQ blend composites with neat Mt and SI-ATRP modified Mt, respectively, was characterized by the X-ray diffractometer X´Pert PRO X-ray (PANalytical, The Netherlands) with a Cu-Kα X-ray source (λ = 1.5418 Å) in the diffraction angle range of 2θ = 5-85°.

1.5 SEM

Morphology of the EPDM/MVQ/Mt systems was characterized by scanning electron microscopy (SEM), using SEM microscope Vega Plus TS 5135 (Tescan, Czech Republic). The specimens for SEM microscopy were prepared as follows: small parts of the samples were cut, submerged in liquid nitrogen for 30 min and then broken while still fully submerged in the liquid nitrogen (in a laboratory-made device) in order to minimize plastic deformations. The resulting samples were fixed by conductive double-adhesive carbon tape on an aluminum support, sputtered with a thin Pt layer (vacuum sputter coater SCD 050 (Leica, Austria) in order to minimize possible charging and e-beam damage, and the fracture surfaces were observed in the SEM microscope at accelerating voltage

30 kV using secondary electron imaging (SEM/SE; the micrographs showed mostly topographic contrast) and backscattered electron imaging (SEM/BSE; the micrographs showed mostly material contrast).

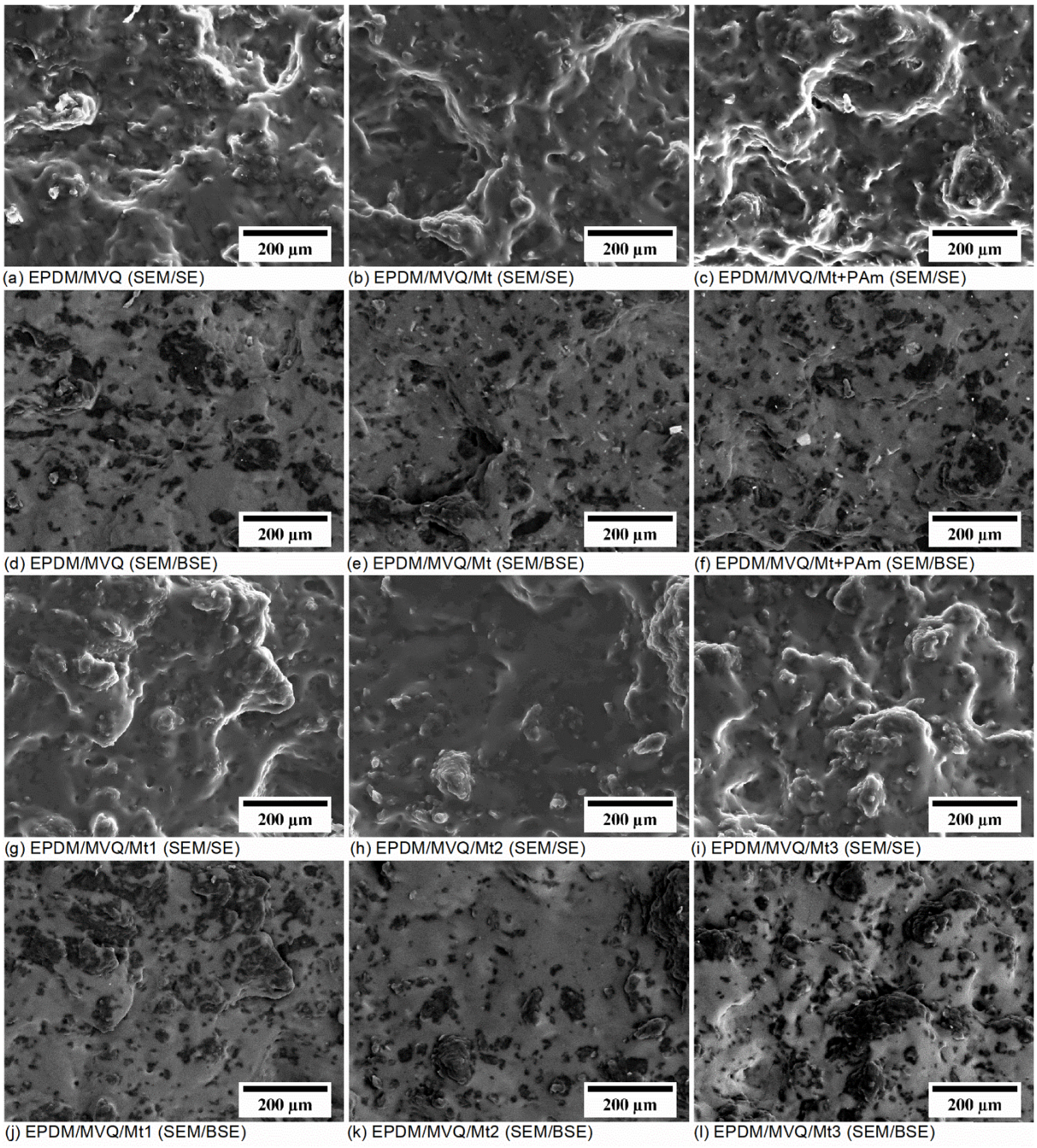

Fig. S1. SEM and SEM/BSE images of EPDM/MVQ blends containing Mt and Mt-*g*-PAm hybrids.

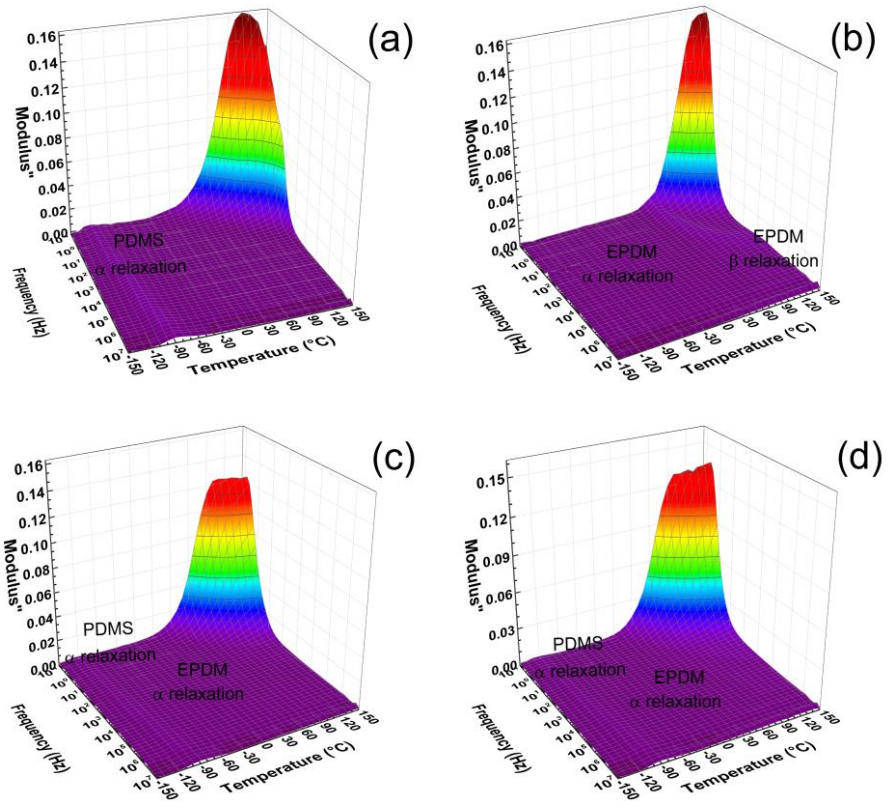

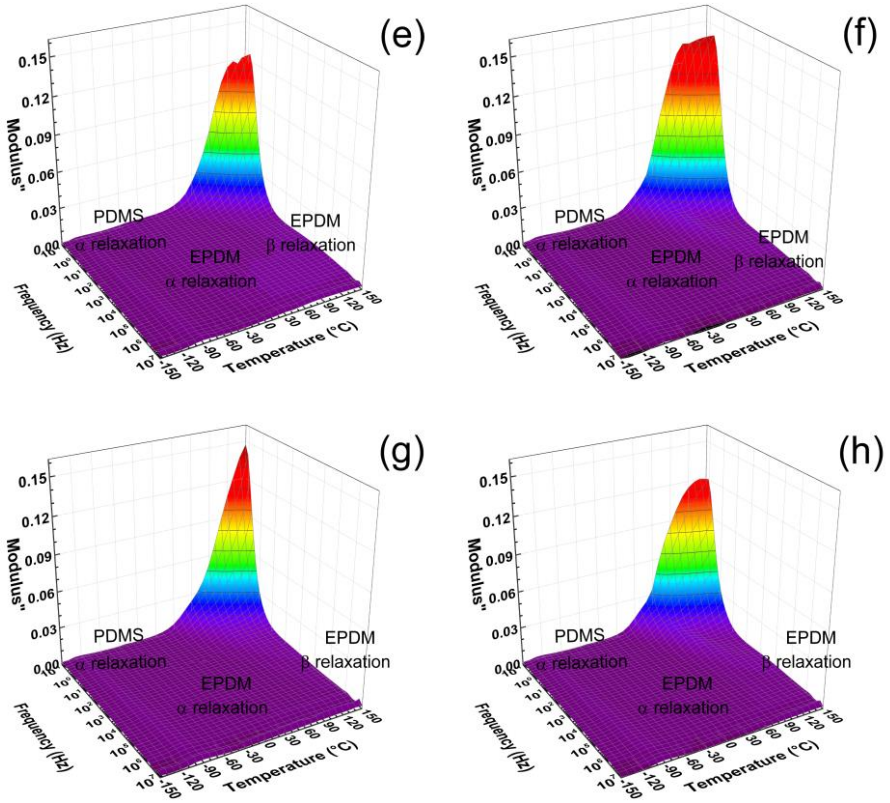

Fig. S2. Dielectric 3D plots of neat MVQ (a), EPDM (b), EPDM/MVQ (c), EPDM/MVQ/Mt+PAm (d), EPDM/MVQ/Mt (e), EPDM/MVQ/Mt1 (f), EPDM/MVQ/Mt2 (g) and EPDM/MVQ/Mt3 (h).

Table S1 Table summarizing parameters of models and activation energies calculated from dielectric data.

Sample name	**VFT α-relaxation MVQ**			**VFT α-relaxation EPDM**			**Arrhenius β-relaxation -COOH**
	τ_0 (s^{-1})	**T_0 (K)**	**B (kJ mol^{-1})**	**τ_0 (s^{-1})**	**T_0 (K)**	**B (kJ mol^{-1})**	**E_a (kJ mol^{-1})**
MVQ	2.10E-11	130	5.5	ND*	ND*	ND*	ND*
EPDM	ND*	ND*	ND*	2.10E-11	160	10.2	49.7
EPDM/MVQ	2.10E-11	118	6.8	2.08E-11	166	10.6	ND*
EPDM/MVQ/Mt+PAm	2.10E-11	124	4.3	2.30E-11	163	10.3	ND*
EPDM/MVQ/Mt	2.10E-11	123	4.7	2.40E-11	163	10.7	ND*
EPDM/MVQ/Mt1	2.10E-11	123	4.7	1.69E-10	168	11.4	51
EPDM/MVQ/Mt2	2.10E-11	123	4.6	1.59E-10	167	9.9	ND*
EPDM/MVQ/Mt3	2.10E-11	123	4.6	2.70E-10	169	11.9	54.6

**ND – not detectable*

References

[1] R. Moucka, M. Mrlik, M. Ilcikova, Z. Spitalsky, N. Kazantseva, P. Bober, J. Stejskal, Electrical transport properties of poly(aniline-co-p-phenylenediamine) and its composites with incorporated silver particles, Chem. Pap. 67 (2013) 1012–1019. https://doi.org/10.2478/s11696-013-0351-7.

[2] F.-M. Preda, A. Alegría, A. Bocahut, L.-A. Fillot, D.R. Long, P. Sotta, Investigation of Water Diffusion Mechanisms in Relation to Polymer Relaxations in Polyamides, Macromolecules. 48 (2015) 5730–5741. https://doi.org/10.1021/acs.macromol.5b01295.